

A.K. Mohamed, M. Lefebvre
(Onera)

E-mail: ajmal_khan.mohamed@onera.fr

Laser Absorption Spectroscopy to Probe Chemically Reacting Flows

Laser absorption spectroscopy is now a well established tool to perform temperature, density and velocity measurements in a wide variety of aerodynamic and combustion flows. Measurements are usually performed on heterogeneous molecules like NO, CO, CO₂ and H₂O which present strong absorption line strengths in the infrared region due to their high dipole moments. In this paper, we present examples of applications using mid-infrared laser diodes in several hypersonic wind tunnels and combustion facilities of Onera and DLR followed by a review of actual developments in new OPO based laser sources providing better coverage of the infrared domain and opening new possibilities of ultra sensitive detection using cavity enhanced or photo-acoustic methods and stand-off distance measurements based on lidar schemes.

Introduction

Laser Absorption Spectroscopy for aerodynamics was developed in the mid 70's using infrared lead-salt diode lasers to probe combustion media [1][2] and has been used in hypersonic flows since the mid 90's [3][4] to probe the free stream in hypersonic facilities like the Onera-F4 hot shot facility [5], the DLR-HEG shock tube [6][7], or the Onera-S4 [6] and Astrium SIMOUN wind tunnels [8]. The technique is based on measuring the absorption intensity of a fast wavelength tuneable laser beam passing through the flow. Velocity, translational temperature and concentration measurements can be derived from the spectral features of molecular absorption lines acquired at high spectral resolution. Measurements are usually performed on heteronuclear molecules like CO, NO and H₂O which are naturally present as a result of real gas effects or as trace pollution species in air flows or on CO₂ in the case of Martian re-entry studies. All of these molecules have strong absorption line strengths due to their high dipole moments and usually the fundamental levels of absorption lines are located in the mid infrared region (wave number > 4 μm), which is well covered by CW lead-salt diode lasers (Figure 1).

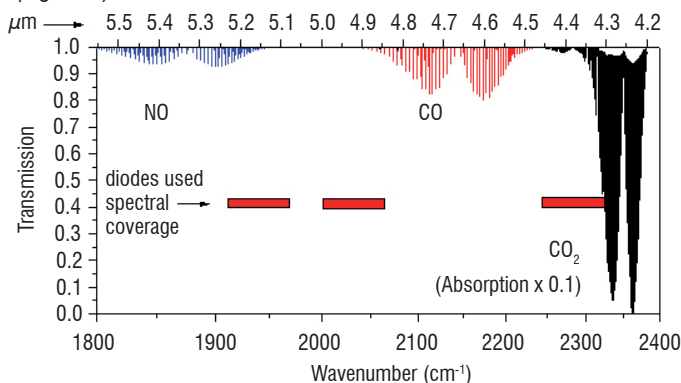


Figure 1- Absorption spectrum of some molecules of aerodynamic interest and spectral emission windows of some of the laser diodes used in wind tunnels and combustion applications.

These lead-salt diode lasers have very narrow line width emissions (around a few MHz or 10^{-3} cm^{-1}) and can be finely tuned (with a resolution close to 10^{-4} cm^{-1}) around absorption lines so that the temperature and pressure broadening can be visualized without any interference broadening from the laser line width itself. This high spectral resolution feature therefore allows temperature measurements from the Doppler line shape on trace molecules in low pressure (less than 1000 Pa) chemically reacting media such as in hypersonic flows where the lines are broadened mainly by temperature effects with typical Doppler line widths of 10^{-2} cm^{-1} . The gas velocity can also be determined from the Doppler shift induced in the line positions of the absorbing species when the beam is not perpendicular to the flow axis. The Doppler shift is of the order of 10^{-2} cm^{-1} at wavelengths around 5 μm for bulk velocities superior to 1000 m/s. Specie density measurements are possible from the integrated intensity of an absorption line if the gas is at Boltzmann equilibrium. Figure 2 illustrates the measurements that can be made from a spectrum presenting an NO absorption line with its Doppler-shifted component for flow conditions indicated in the figure. The unshifted line results from absorption of molecules at low velocities in the boundary layer of the flow or which are diffused outside of the flow.

Such measurements can be made at repetition rates up to 10 kHz which is fundamental to probe high enthalpy facilities with short duration flows (200 ms for Onera F4 and a few ms for DLR HEG) and where the aerodynamic conditions change quickly in the order of a few percent per ms. Lead-salt diode lasers are good at performing these high speed measurements as well as emitting in the mid-infrared to probe molecules of aerodynamic interest. However, one main drawback is that cryogenic technology (usually liquid nitrogen cooling) must be used to cool these diodes operating around 100K and as well as the HgCdTe detectors for optimal performance in the mid-infrared. Up to now, non-cryogenic instruments using visible or near infrared diodes have been limited to H₂O, or atomic species like Rubidium or Potassium which must be seeded beforehand in the flow [7].

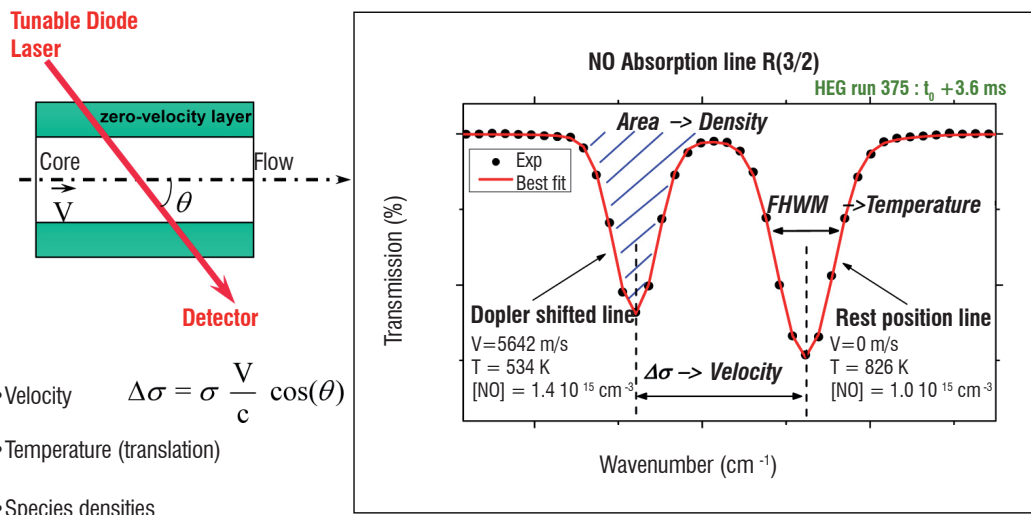
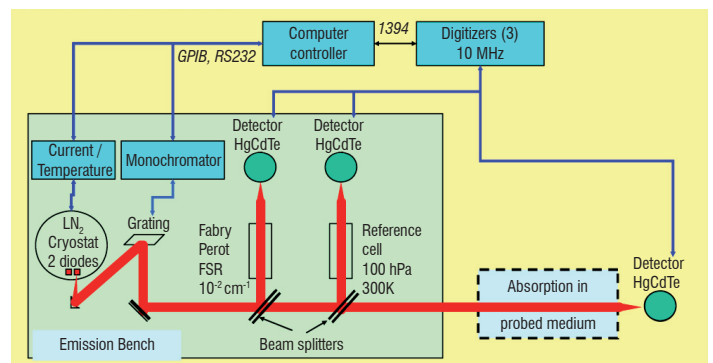


Figure 2 - The usual parameters which can be deduced from pressure-free absorption lines (Velocity is determined with an accuracy of about 5% whereas temperature and density have accuracies around 10%)

Fortunately, recent developments in new laser sources (Quantum Cascade Lasers [9], Interband Cascade Lasers [10], GaSb DFB laser diodes [11], OPO [12],...) now allow us to consider non-cryogenic setups (at least for the laser emission part) to probe the molecules of aerodynamic interest on their most absorbing lines in the infrared domain. Advances in cavity enhanced techniques [13](CRDS, ICOS,...) that improve the sensitivity of detection also offer new possibilities for probing some of these molecules in the visible or near infrared region with room temperature lasers.

Diode laser absorption spectroscopy in windtunnels

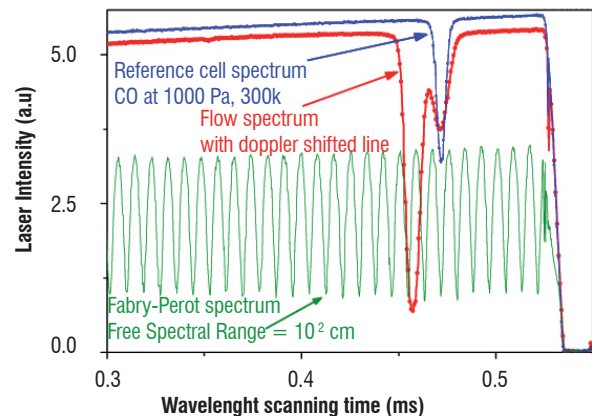
A typical diode laser absorption spectrometer (DLAS) is presented in Figure 3a. Such an instrument is composed of a laser emission head, photo-detectors and fast digitizers to convert and record the signals from the photo-detectors. For operations in the mid infrared domain, the diode laser emission head is in the form of a liquid nitrogen cooled cryostat containing one or two lead-salt diodes operating near 100 K. Nowadays Quantum Cascade lasers (QCL[9]) working in CW mode can also be used in the same cryostats. Stabilized current generators are used to control the diode temperature and current more finely for the required laser emission. A 500-mm focal length monochromator and optical collimating components are used to filter a single mode out of the emission spectrum of the diode and collimate the output laser light into a beam of about 15-mm diameter. About 30% of this beam is deviated for wavelength and intensity calibrations using a 0.00975 cm^{-1} free spectral range confocal spherical Fabry-Perot etalon and a reference cell filled with the gas to be probed at a few hundreds of Pascal. All these elements are grouped on an optical bench 1.5 m long and 0.8 m wide. The rest of the laser beam exiting this bench is then made to cross the gas medium to be studied with the help of mirrors before measurement of its intensity on a third photo-detector. Figure 3b presents a set of three absorption spectra (two for calibration and one for the medium being probed) which is typical when performing measurements with this instrument. The spectra are obtained through tuning the wavelength over about 1 cm^{-1} in a time interval of 1 ms. Figure 4 shows a typical experimental arrangement which is usually used in the Onera F4 wind tunnel.



a) Spectrometer main features

TDLAS raw spectra example with a diode for CO probing (CO line at 2055.6 cm^{-1} used to perform velocity measurements)

Three simultaneous channels (two for calibration : intensity and wavelength)
Spectra acquired in 1 ms (at repetition rate 1 kHz)



b) Examples of acquired spectra

Figure 3 : Typical DLAS spectrometer

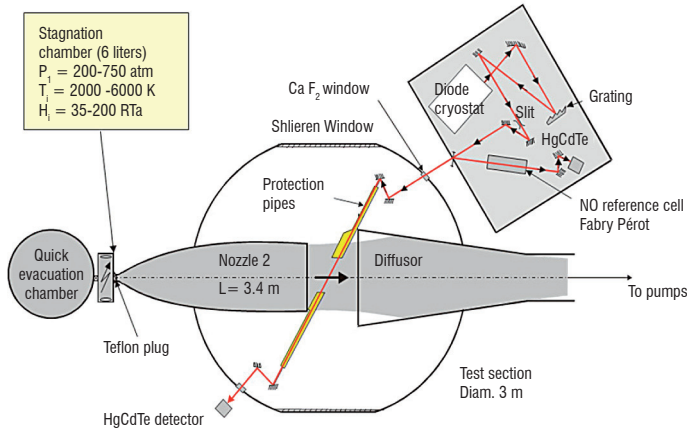


Figure 4 - Typical DLAS set up in the F4 wind tunnel. The laser emission bench and the optical detection setup are outside the vacuum chamber. The laser beam enters the vacuum chamber through CaF_2 windows and crosses the flow at the smallest possible angle to the flow's axis, so as to induce the largest Doppler shift for velocity measurement purposes.

Data reduction

After wavelength and intensity calibration with the help of the calibration channels (Figure 3b), the useful segment of each corrected spectrum is matched to simulated spectra through an iterative non-linear least-squares fitting procedure [14] to retrieve the velocity, the kinetic temperature, and the concentrations of the absorbing species. The simulated spectrum is constructed from the classical Beer-Lambert absorption law. In a homogeneous medium, the attenuation of the beam intensity $I(\sigma)$ is thus described by:

$$I(\sigma) = I_0(\sigma) \exp[-S_x \cdot f(\sigma, \sigma_x) \cdot N \cdot L]$$

where $I_0(\sigma)$ is the initial intensity of the beam, N the density of the absorbing molecules, L the absorption path length, and S_x the absorption strength of the line centered at position σ_x . The function $f(\sigma, \sigma_x)$ is the normalized absorption line shape which takes into account all types of line broadening around the center wave number σ_x . Because of the high resolution achievable here, there is no line broadening due to the instrument used; the line profile is described solely by thermodynamic and molecular parameters of the medium. It is, in most cases, a Voigt function which is itself a convolution of a Doppler profile f_D with a Lorentz profile f_L . The Doppler profile describes broadening due to thermal motion of the molecules at the kinetic temperature, T :

$$f_D(\sigma - \sigma_x, T) = \frac{1}{\sqrt{\pi} \alpha_{xD}(T)} \cdot \exp\left[-\left(\frac{\sigma - \sigma_x}{\alpha_{xD}(T)}\right)^2\right]$$

with the half-width at half maximum (HWHM) of the absorption expressed in cm^{-1} as:

$$\alpha_{xD}(T) = \sqrt{\ln(2)} \frac{\sigma_x}{c} \sqrt{\frac{2 \cdot k_B T}{m_{\text{molécule}}}} = 3.58 \cdot 10^{-7} \sigma_x \sqrt{\frac{T}{M}}$$

where k_B is the Boltzmann constant and M is the molar mass. The Lorentz profile represents line broadening due to collisions. It depends on the pressure P and the kinetic temperature of the medium:

$$f_L(\sigma - \sigma_x, P, T) = \frac{1}{\pi \cdot \alpha_{xL}(P, T)} \cdot \frac{1}{1 + \frac{(\sigma - \sigma_x)^2}{\alpha_{xL}^2(P, T)}}$$

with HWHM given in cm^{-1} as:

$$\alpha_{xL}(P, T) = \alpha_{xL}^0(P_0, T_0) \frac{P}{P_0} \left[\frac{T_0}{T}\right]^{y_{lor}}$$

The coefficients $\alpha_{xL}^0(P_0, T_0)$ and y_{lor} are derived either from quantum mechanics or through experiments. In our case, we use the values of y_{lor} ($=1.5$) and $\alpha_{xL}^0(P_0, T_0)$ from the HITRAN database [15], tabulated for a reference pressure $P_0 = 1$ atmosphere and temperature $T_0 = 296$ K.

In a flow with bulk velocity v , the center line wave number σ_x will be Doppler-shifted to $\sigma_x - \Delta\sigma_x$ with

$$\Delta\sigma_x = \sigma_x \frac{v}{c} \cos(\theta),$$

where θ is the angle between the laser beam and the flow axis, and c is the speed of light. In this case, the line shape has to be calculated from this shifted wave number $\sigma_x - \Delta\sigma_x$.

In a medium in thermodynamic equilibrium at T , the quantum mechanical expression of the line strength S_x is given as

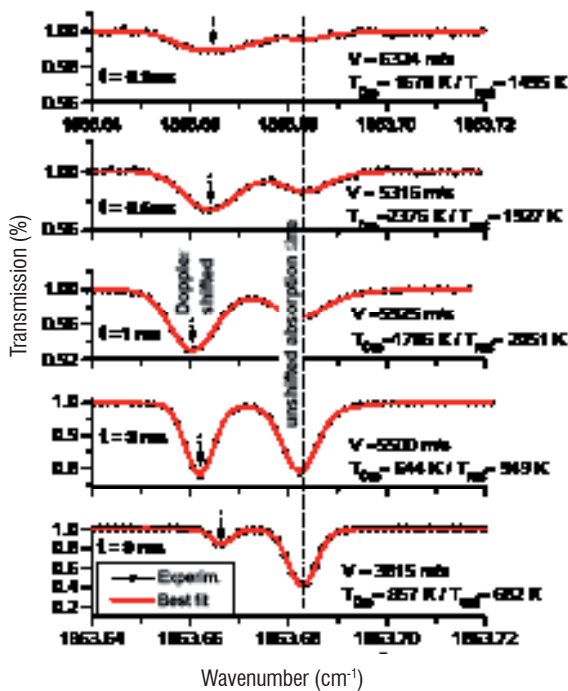
$$S_x(T) = S_x(T_0) \cdot \frac{Q_x(T_0)}{Q_x(T)} \cdot \frac{1 - \exp\left[-\frac{hc \sigma_x}{k_B T}\right]}{1 - \exp\left[-\frac{hc \sigma_x}{k_B T_0}\right]} \cdot \exp\left[-\frac{E_x}{k_B} \left(\frac{1}{T} - \frac{1}{T_0}\right)\right]$$

where h is Planck's constant. $S_x(T_0)$ is determined experimentally or calculated at $T_0 = 296$ K [15]. $Q_x(T)$ is the partition function, E_x the molecular low-energy transition x absorbing at wave number σ_x .

Typical measurement results in high enthalpy wind tunnels

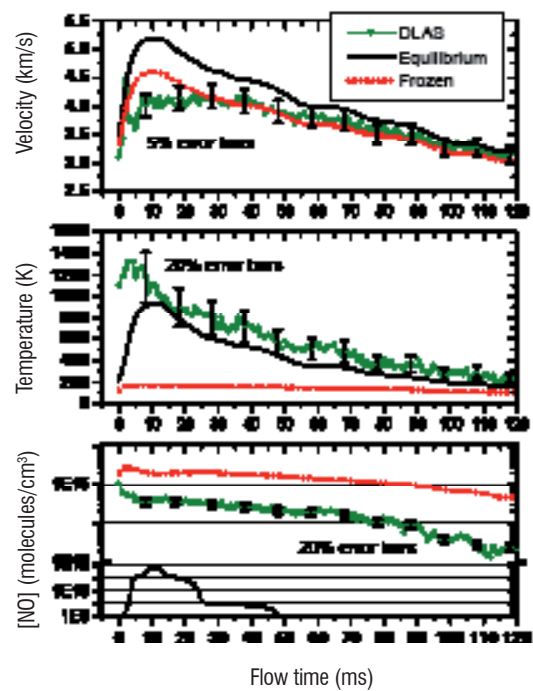
A simple two-layer model is usually assumed for the flow generated in high enthalpy wind tunnels. One layer corresponds to the flow core, with a constant free stream velocity V . The other layer (called the external layer) includes all of the gases outside the flow core with no bulk velocity that contribute to rest-position lines in the absorption spectrum. Figure 5a shows a series of spectra acquired at different times during a run together with the corresponding best fitted simulated spectra inferring the values for velocity, temperature and NO

Diode laser Absorption Spectra
HEG run 375



a) Typical flow absorption changes during a run at the DLR HEG shock tube monitored on the NO (R3/2) line [6]. The acquired spectra are matched to simulated ones to infer values for velocity, temperature and NO density

DLAS temperature, velocity and [NO]
F4 Run 762 condition III (50 MPa; 15 MJ/kg)



b) Changes over time in parameters deduced from acquired spectra for a run at the Onera F4 wind tunnel. The measured values are compared to two series of results from CFD calculations Equilibrium and Frozen hypothesis[16][17])

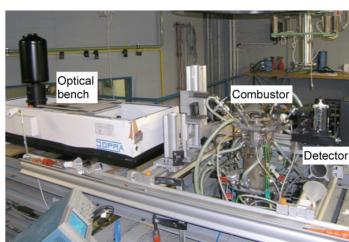
Figure 5 – Example of DLAS measurement results in high enthalpy wind tunnels

density. Only the spectral window around an NO line is presented. The parameter values derived from the processing of successive spectra are traced in Figure 5b and can be used to follow the time variations of such transient flows usually occurring in high enthalpy wind tunnels. In Figure 5b, the measured values are compared to two series of results from CFD calculations [16][17] assuming either ‘equilibrium conditions’ (where, using the temperature parameter example, vibrational temperature is equal to the kinetic temperature) or ‘frozen conditions’ (where the vibrational temperature remains at much higher values than the kinetic one and close to the temperature before expansion along the nozzle).

Measurements of aero engine effluents

We illustrate here the potential of laser absorption spectroscopy measurements on aero engine effluents through experiments performed in the framework of a European research project, MENELAS (Minority effluent measurements of aircraft Engine emissions by infrared Laser Spectroscopy [18]), carried out by a consortium of several aerospace institutes and laboratories led by Onera. The techniques which

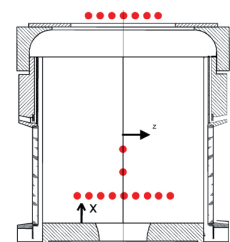
were under development were MIDROPO (Mid-infrared Doubly Resonant Optical Parametric Oscillator), Mid-infrared Pico-second LIDAR (MIRPL) and tunable diode laser absorption spectroscopy (DLAS). The latter was considered to be the technique with the highest maturity, which was ready to undergo field experiment demonstrations during the project's lifetime. The demonstrations were performed with a model gas turbine combustor in the DLR premises in Köln and on the exhaust gases of Cessna Citation II research aircraft at a test site at Amsterdam Airport Schiphol. An adapted version of the DLAS wind tunnel equipment already described above was deployed to probe CO, CO₂, NO and H₂O during these two demonstrations. The experimental set up for the model combustor is presented in Figure 6. As the model combustor had optical access, the technique was not only used to measure at the outlet but inside the combustor as well. Fast fluctuations in the flow with a time scale of less than 1 ms were observed (Figure 7a) for the measurements. In order to reduce these effects on the spectra acquisition, the spectrometer was set to conduct measurements at a f=10 kHz repetition rate. This optical measuring technique provides integrated values along the line of sight of the laser beam.



a) DLAS instrument at DLR testbed

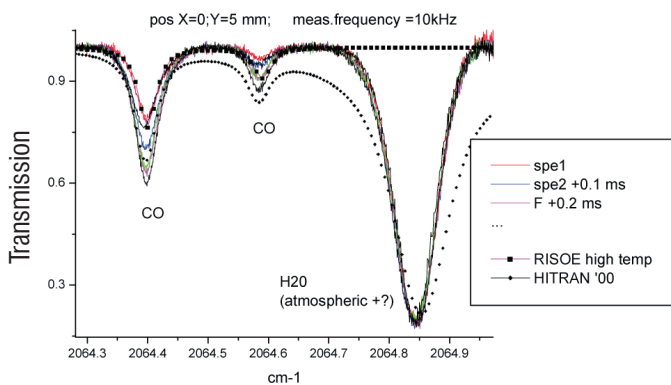


b) Combustor in operation

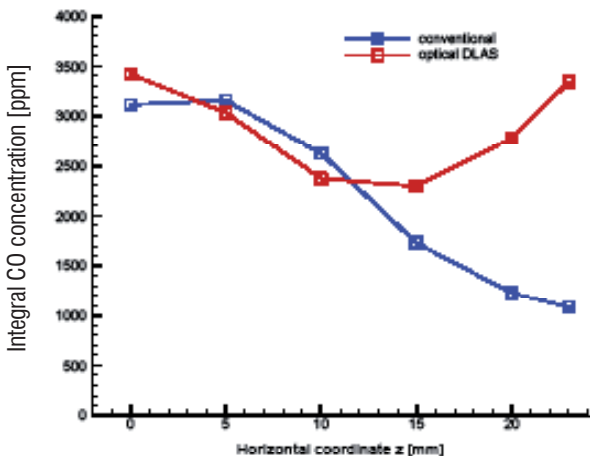


c) Positions of optical measurements inside and at the outlet of the combustor

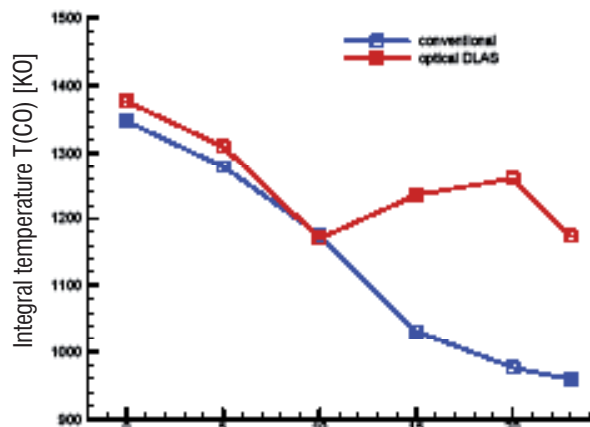
Figure 6 – DLAS experimental setup on a DLR combustor (Courtesy DLR Köln[19])



a) Examples of absorption spectra in the combustor



b) Horizontal profile of integral CO concentrations at $x=10$ mm inside the combustor at $T_3=850$ K and $T_f=2000$ K



c) Horizontal profile of integral temperatures weighted with the CO concentration at $x=10$ mm inside the combustor at $T_3=850$ K and $T_f=2000$ K

Figure 7 – Examples of DLAS results for the DLR combustor (T_3 : air preheat temperature; T_f : Flame temperature; detailed description is given in reference[19])

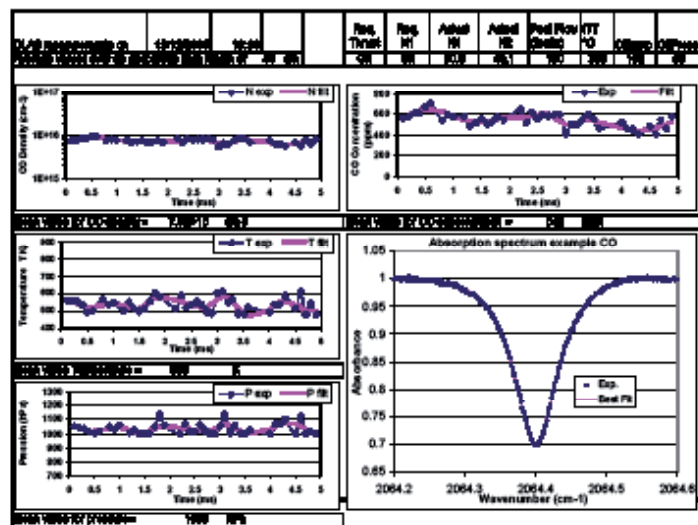
Therefore integral values had to be calculated [19] from the spatially resolved measurements with conventional techniques to allow a comparison with the optically measured data. Figure 7 (b,c) presents two comparative examples of temperature and CO concentration horizontal profiles. There is a good agreement with a deviation of about 10 % near to the flow axis whereas large differences, which are yet to be explained, appear close to the wall of the combustor.

The experimental setup for the second field experiment carried out during the MENELAS project is depicted in Figure 8a. The spectrometer was put in a van type vehicle placed at a distance of approximately 4 meters from the probed zone and mirrors mounted on poles near the engine were used to direct the laser beam so that it crossed the flow vertically at a distance of 80 cm downstream of the engine outlet. Only measurements on CO and H₂O were tried during the time window allowed for the experimental campaign. A few examples of results obtained are presented in Figure 8b for a set of successive spectra acquired at 10 kHz during 6 ms for engine thrust settings at 30% of maximum power (other details can be found in reference [20]).

These MENELAS experiments demonstrated that infrared laser absorption spectroscopy has the potential for fast and high spatial resolution measurements of combustion species. However, some future development work on more rugged equipment is still needed as the goal is to replace the gas analysis currently performed with intrusive probe measurements in order to fulfill ICAO standards for engine emission measurements and to help us understand the combustion processes in a gas turbine.



a) Set up at the NLR test site



b) Examples of measurements

Figure 8 – DLAS measurements on the exhaust gases of the NLR's Cessna Citation II research aircraft at a test site at Schiphol Airport Amsterdam (Courtesy NLR)

Prospects

The use of mid-infrared diode lasers has been a great help in the development of absorption spectroscopy for applications in different flow media in aerodynamics and combustion. The trend now is to develop low cost setups with non-cryogenic semiconductor lasers

(QCL [9] in the mid IR, interband cascade lasers (ICLs [10]) and GaSb DFB diode lasers [11] in the 2-3 μm range) for less cumbersome and more routine use of this technique. Moreover, the beams from such lasers can be more easily collimated and open up new possibilities for fiber-optic coupling. This can help to protect the beam up to the edges of the flow thereby reducing the interference caused by diffused molecules outside of the flow. The fiber optic possibility also allows for the use of miniature probes which can be placed inside the flow for localized probing.

However, semiconductor lasers emit only on limited spectral windows and are of low power. Fortunately development in non linear optics now offers the possibilities of new laser sources (OPO [12]) with high

brightness and wide spectral coverage in the mid-infrared spectrum. (see box 2).

Other improvements which may offer new possibilities for the laser absorption technique are:

- Use of several laser beams at different wavelengths for simultaneous measurements on several species
- Flow tomography coupled with Abel inversion through the use of several laser beams or quick spatial scanning of a single laser beam
- Use of multi-pass or CRDS methods to enhance sensitivity (see box 1): this can help with the probing of very weak absorption lines (like that for O_2) or can allow for short absorption lengths, with the aim of building miniature probes placed in a flow for more local measurements

Box 1 - High Speed Cavity Ring-Down Spectroscopy

CRDS is a laser-based absorption spectroscopy technique which directly deduces the absolute value of optical losses in a high finesse optical cavity from its photon lifetime [O'keefe]. The ring-down cavity is created by positioning two highly reflective mirrors ($R > 99.99$) around the gas medium of interest. The light source is coupled to the ring-down cavity, resulting in a rapid buildup of the intensity of radiation trapped inside. After abruptly stopping the laser injection, the stored light propagates back and forth within the cavity and, at each pass, gradually leaks out through the mirrors. The transmitted intensity $I(t)$ is an exponential decay of the initial intensity I_0 given by the equation

$$I(t) = I_0 \exp(-t / \tau) \quad (1)$$

where τ is the ring-down time of the cavity. The loss rate per distance is then given by

$$\frac{1}{c\tau} = \frac{1-R+A}{L} + \alpha \quad (2)$$

with c the speed of light, L the cavity length, R the reflectivity of the mirrors, A the diffraction losses of the mirrors, and α the medium absorption coefficient. A plot of the loss rate α as a function of the laser frequency is a CRDS spectrum. The absorption loss profile is directly proportional to the chosen absorption line profile from which one can deduce the specie concentration, as well as the temperature, pressure and velocity in gas flows. CRDS has originally been developed with pulsed laser sources [O'keefe] but has since been proven to work with continuous-wave lasers as well [Romanini]. The basic principle of a cw-CRDS setup is illustrated in Fig. B1-01.

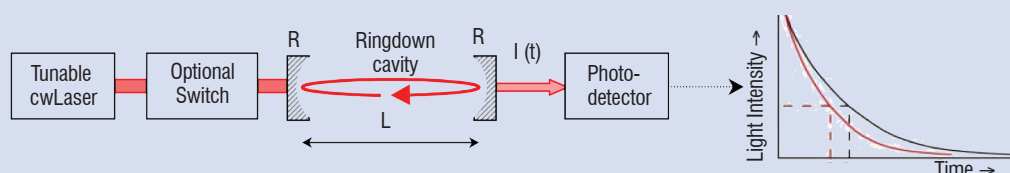


Figure B1-01. Diagram of a typical ring-down setup that produces an exponential decay of the transmitted light after termination of the laser coupling. An optional acousto- or electro-optic switch is generally used to interrupt injection by cw laser sources and prevent further entry of light. τ_0 and τ

Compared with traditional single or multi-pass absorption methods, CRDS exhibits the advantages of long effective absorption path lengths (many kilometers) combined with intrinsic insensitivity to source-intensity fluctuations, thus offering a great sensitivity which already been exploited in a wide variety of fields. But the measurements times using a standard scheme are usually relatively long in the order of seconds if not minutes due the laser wavelength positioning and optical switching for a clean exponential decay in the cavity.

Improvements in the measurement speed are therefore required to enable fast and sensitive analysis of transient flows such as those generated in blow-down hypersonic wind tunnels. Indeed, the flows we are targeting are generated during short gusts, typically lasting a few 100-ms, with aerodynamic conditions changing by a few % per ms. A scheme allowing the measurement of an absorption line within time period of a ms is therefore required (shorter times are sought to combat fluctuations in combustion flames). Another difficulty arises from the low pressure nature of the gas met in wind tunnels, usually of a few mbar presenting absorption line widths essentially due do Doppler broadening and which are at one tenth smaller than those at atmospheric pressure (Lorentz broadening).

It has already been demonstrated that, in conventional cw-CRDS, a rapid extinction of the laser beam, enabling a free exponential photon decay is possible without any optical switch using only a fast sweep either for the cavity length at fixed laser frequency [He1], or for the laser frequency over the motionless cavity modes [He2]. In both cases, a partial build-up of the intra-cavity energy rapidly occurs as soon as the resonance condition between the laser frequency and a cavity mode is satisfied. The subsequent light exponential decay is observed as the laser frequency and the cavity mode come out of resonance. However, to get a decent signal to noise ratio, averaging procedures have to be applied on the signals thus giving long integration times. At Onera, we further developed the fast laser sweep concept with low noise avalanche photo-detectors and were able to reduce the acquisition time of an exploitable absorption profile to 2 ms with a repetition rate of 250 Hz compatible with our wind tunnel application [Debecker].

In the case of a rapid laser frequency sweep on a static cavity of length L , the maximum achievable frequency resolution corresponds to the free spectral range (FSR), which is $FSR_{static} = 1/2nL$, in spectroscopic cm^{-1} units with n the refractive index approximated to one and henceforward discarded. As an example, for a 50-cm-long cavity, the separation between ring-down events is $0.01 cm^{-1}$ (0.3 GHz). In flows simulating reentry conditions at high altitudes, this resolution is insufficient to probe low pressure absorption line widths (or Doppler shifts for velocity measurements) which are of the order of $0.05 cm^{-1}$. We present below two ways we investigate how to improve spectral resolution in high speed cw-CRDS designs.

CRDS spectral resolution enhancement by simultaneous laser and cavity tuning

One way to enhance spectral resolution involves simultaneous laser and cavity tuning. In order to increase the number of recorded ring-down events, the cavity resonance mode frequencies (V_{mode}) must be synchronously swept in the opposite direction to the laser mode (V_{λ}). This leads to an increased number of frequency-matched events between the laser and the cavity, giving ring down points separated by a spectral interval smaller than the FSR of the static cavity as shown in Figure B1-02. An experimental result on an O_2 line at high and low pressure is presented in Figure B1-03.

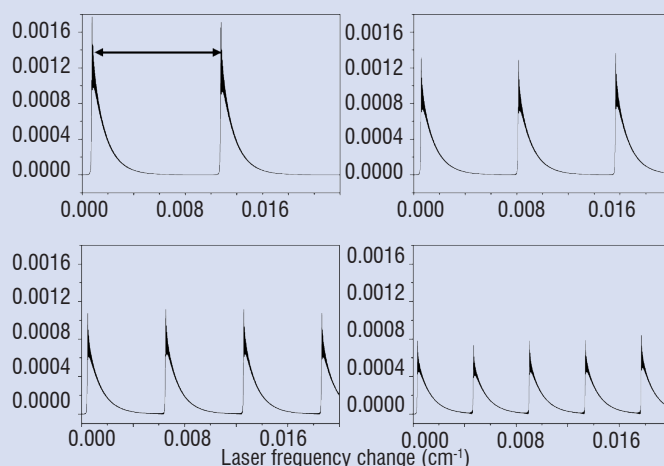


Figure B1-02 – Increased ring-down events for simultaneous cavity and wavelength tuning ($0.4 cm^{-1}$ in 2 ms)

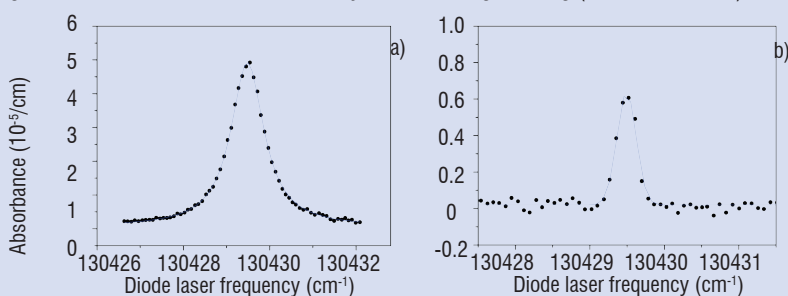


Figure B1-03. Absorption spectra for O_2 in air, recorded during a 280-Hz laser frequency-sweep and a synchronous $5\text{-}\mu m$ cavity modulation range. (a) At atmospheric pressure, a Lorentzian profile of $0.095\text{-}cm^{-1}$ -FWHM is superposed to the experimental points. (b) At 20 mbar, a $0.025\text{-}cm^{-1}$ -FWHM Gaussian profile provides a fit of the plotted points.

The spectral resolution enhancement factor can be derived from the expression of the dynamic FSR for a moving cavity [Debecker]:

$$FSR_{dynamic} = \frac{1}{2L - 2\lambda \frac{V_L}{V_{\lambda}}} \quad (3)$$

where V_{λ} and V_L are the linear scanning velocities respectively for laser wavelength and cavity length tuning. The velocity for a resonance mode of the cavity is expressed as $V_{mode} = -\lambda V_L / L$ and must therefore be of opposite sign to V_{λ} for spectral resolution enhancement.

The denominator in equation (3) presents all of the parameters to tune for resolution enhancement. Fig. B1-04a illustrates one of the possibilities, namely the influence of cavity length scanning velocity V_L while other parameters are fixed at the values $\lambda = 0.766 \mu\text{m}$, $L = 0.5 \text{ m}$, $V_\lambda = 0.2 \text{ cm}^{-1}/\text{ms}$ corresponding to one of our experimental setups described in reference [Debecker]. Fig. B1-04b shows that the resolution enhancement increases with shorter cavities, which is quite welcome in the task of miniaturizing a CRDS device.

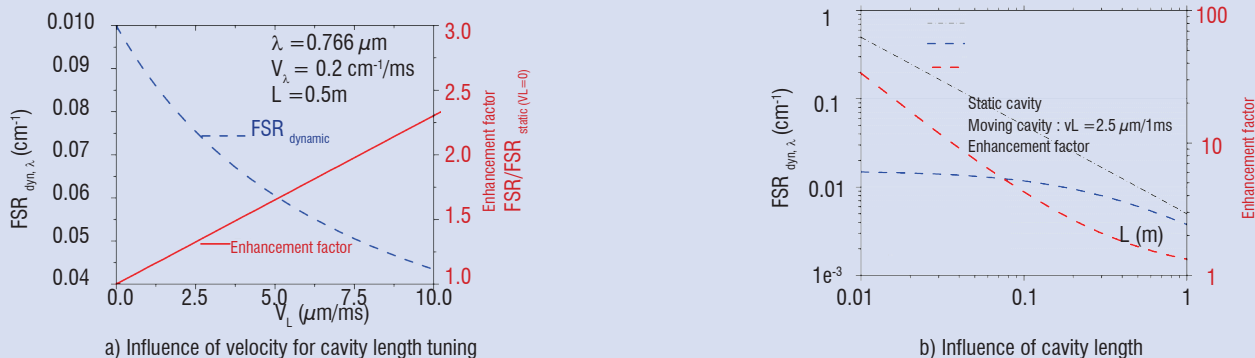


Figure B1-04- Dependence of the dynamic FSR and the enhancement factor of spectral resolution on the cavity length tuning speed.

CRDS spectral resolution enhancement using transverse modes

Another scheme we investigated for increasing spectral resolution during a rapid scan of the laser wavelength is based on the use of a cavity's transverse mode structure. But the straightforward use of the different mode orders leads to quite noisy absorption line profiles because of mode overlapping and also due to the fact that each transverse mode exhibits a distinct decaying coefficient. This is because each mode has a distinct spatial overlapping pattern with the mirrors' surfaces which are generally not homogeneous in reflectivity. However, these problems can be circumvented through off axis injection (Fig. A5). By choosing a proper ad hoc cavity length, called the "magic length", the continuum comb of the TEM_{mn} cavity structure modes encountered by an incoming plane wave is converted into a fractionally degenerate mode structure. For a particular length, the "magic length", therefore is a finite number N of the family of degenerate modes within an FSR on-axis of the cavity. This factor N also defines the number of cavity round-trips before the spatial beam overlapping leading to an effective $\text{FSR}_{\text{off-axis}} = \text{FSR}_{\text{on-axis}}/N$ thereby increasing the spectral sampling by a factor of N . The cavity's length can be imagined as having been stretched by the factor N . There is no overlapping between individual transverse modes and the same surfaces of the mirrors are seen by all the groups of degenerate modes leading to absence of mode-to-mode fluctuations and hence quite smooth absorption profiles. Moreover, this injection scheme is also useful for attenuating the ringing effect usually observed with on-axis injection [Courtois].

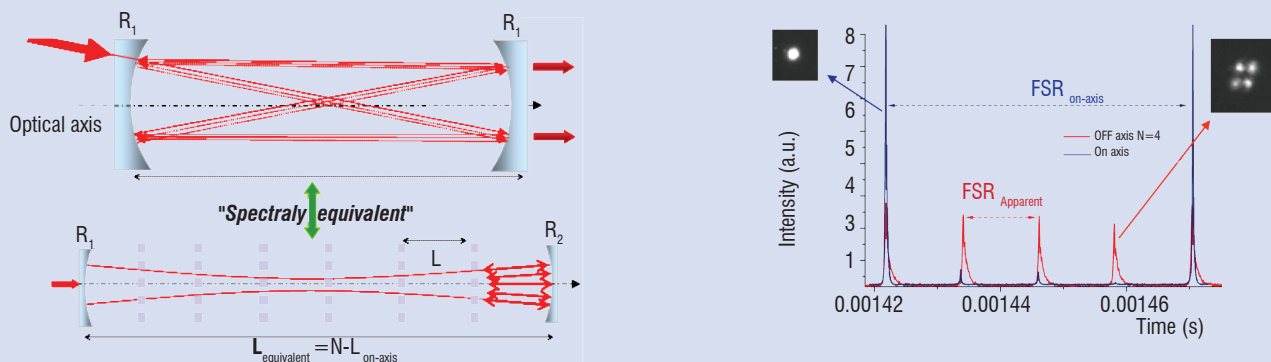


Figure B1- 05 - (Left side) Off-axis injection principle with below its on-axis spectral equivalence. (Right side) Comparison between TEM₀₀ on-axis injection (Excitation of first transverses modes can be observed on the figure) and $N=3, K=1$ (i.e same cavity size) off-axis injection of the cavity. Because in off-axis (for discrete round trip Gouy phase value) light spatially overlaps on itself after N round trips (red ring down events), apparent FSR is divided by N . Since one resonance leads to one point on the profile, spectral resolution is increased by a factor N .

[O'Keefe] A. O'KEEFE AND D. A. DEACON - *Cavity ring-down optical spectrometer for absorption measurements using pulsed laser sources*. Rev. Sci. Instrum. 59, 2544-2551 (1988).

[Romanini] D. ROMANINI, A.A. KACHANOV, N. SADEGHI, AND F. STOECKEL - *CW cavity ring-down spectroscopy*. Chem. Phys. Lett., 264, 316-322 (1997).

[He1] Y. HE AND B. J. ORR - *Optical heterodyne signal generation and detection in cavity ring-down spectroscopy based on a rapidly swept cavity*. Chem. Phys. Lett., 335, 215-220 (2001).

[He2] Y. HE AND B. J. ORR - *Rapid measurement of cavity ring-down absorption spectra with a swept-frequency laser*. Appl. Phys. B, 79, 941-945 (2004).

Box 2 - New laser sources for absorption spectroscopy

Most lasers have a frequency tuning range which is restricted to a small fraction of the frequency gap between the quantum levels connected by the laser radiation. This rather limited wavelength tunability has restricted the potential use of the main lasers to only a few applications of spectroscopy. Indeed, in order to address the fundamental absorption lines of most molecular species, a laser source that provides wide tuning over the mid-infrared domain (2-10 μm) is needed. Among the potential laser sources, there are quantum cascade lasers and parametric devices. Here, our interest is mainly focused on parametric devices which are very promising for spectroscopy due to their very broad tunability.

Parametric devices are wavelength converters based on a second order nonlinear optical process. Basically, the frequency conversion is obtained by illuminating a nonlinear crystal with a laser beam at a given frequency (ω_p), see Figure B2-01. The crystal acts as a gain medium for the production of two waves called signal and idler, respectively at frequencies ω_s and ω_i such that $\omega_p = \omega_s + \omega_i$, this relationship expresses the conservation of the photon energy which is a specific property of any parametric process. Because the parametric conversion is not a resonant process, the possible values of the signal and idler frequencies do not depend on the discrete energy levels of the nonlinear medium, in opposition to a laser medium. Indeed, ω_s and ω_i are determined by the conservation of momentum or phase matching condition $k_p = k_s + k_i$ where k_j is the wave vector of the wave j . Given that each wave vector depends on the refractive index of the medium, the signal and idler frequencies can easily be tuned by changing the propagating conditions of the three waves through the nonlinear crystal yielding a frequency tuning range that is limited only by the optical dispersion of the index of refraction and the optical transmission of the nonlinear crystal.

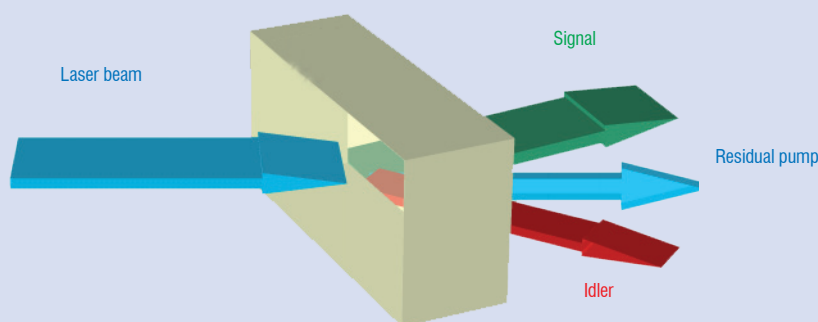


Figure B2 - 01 - Illustration of the parametric conversion process

Two main approaches for adjusting the output wavelengths are now well developed. The first one uses a birefringent crystalline medium where the phase matching condition and subsequently the ω_s and ω_i frequencies are obtained by selection of the waves' polarizations, crystal orientation and/or temperature adjustment. The second one uses a micro-structured nonlinear medium to compensate the optical dispersion of the material periodically. In which case, the momentum conservation is obtained in a quasi-phase matching approach where the optical wave vectors are related to the grating vector of the periodic structure (k_G) by $k_p = k_s + k_i + k_G$, where $|k_G| = 2\pi / \Lambda$, Λ is the grating period. Most of commercial quasi-phase matched crystals are produced with ferroelectric materials (lithium niobate, lithium tantalite, ...) where the ferroelectric orientation has been periodically poled in opposite directions by using an electric-field poling technique, see Figure B2-02. Such a technique allows the nonlinear material to be engineered for the desired output wavelengths by choosing the poling period. The signal and idler frequencies can be tuned around the central wavelength, which is fixed by the poling period, by adjusting the crystal's temperature.

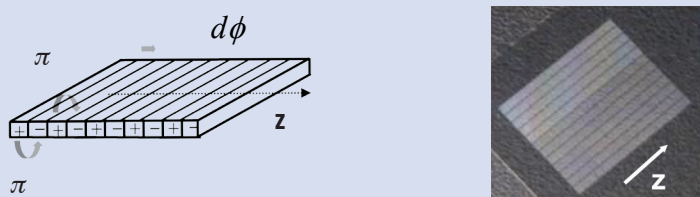


Figure B2 - 02 - Principle of the quasi-phase matching technique (left) and picture of a commercial periodically poled crystal comprising 12 parallel gratings

Parametric devices based on birefringent or quasi-phase matched crystals are able to convert a fixed pump frequency into a pair of widely tunable mid-infrared radiations that can be used for spectroscopic applications. Nonetheless, the simplest architecture based on a pump laser followed by a non linear crystal cannot provide the required specifications for most spectroscopic applications. Firstly, the parametric conversion efficiency is rather low and therefore, after only one pass through the non linear crystal, the available energy is usually too limited for high sensitive gas sensing. Secondly, the band width of the parametric gain curve is relatively broadband (10 cm^{-1} or more) leading to signal and idler line widths that are too broad for spectroscopic applications which require a line width of less than 0.01 cm^{-1} .

To overcome these two limitations, two approaches have been developed. The first one is based on difference frequency generation (DFG). Basically, DFG-systems use a mid-IR narrow band radiation which is obtained by mixing a pump laser beam and a tunable diode laser, usually working in the telecom band, through a nonlinear crystal. This approach has been mainly used in the continuous wave regime with a multipass cell in order to perform high sensitive DFG-spectrometers. The main advantage of DFG-spectrometers results from their simplicity, however the range of applications is limited by the availability of tunable diode lasers and the low output power level available after DFG. The second approach is based on optical parametric oscillators (OPOs). In this case, the nonlinear crystal is placed within an optical resonator, taking advantage of multiple round-trips through the parametric gain medium.

The simplest OPO scheme is based on an optical resonator which is resonant at only one wavelength (signal or idler, exclusively). Singly resonant OPO provides good conversion efficiency ($> 10\%$) and can deliver a narrow line width by inserting intra-cavity dispersive elements or by injection-seeding the optical resonator with an external laser source. However, the introduction of dispersive elements (diffraction grating, Fabry Perot etalon) increases the optical losses of the resonator and consequently the threshold of oscillation of the OPO whereas the injection seeding technique reduces the spectral range of the OPO to the seed source tunability. These two limitations can be circumvented by using an optical resonator where both the signal and idler radiations are resonant in two separate cavities, see Figure B2-03. As has been demonstrated at Onera, a dual-cavity doubly resonant OPO can oscillate on a single longitudinal mode with a low threshold of oscillation. For reasons of compactness, the dual-cavity doubly resonant OPO developed at Onera is based on two entangled cavities where four mirrors are placed symmetrically on each side of the non linear crystal, see Figure B2-03. The signal and idler waves oscillate between pairs of mirrors M1-M3 and M2-M4, respectively. The inner mirrors (M1, M4) are deposited onto the crystal faces whereas the external mirrors (M2, M3) are mounted on two PZT actuators for fine frequency tuning. The radii-of-curvature of external mirrors are chosen to optimize the mode overlapping between the two cavities and the pump beam.

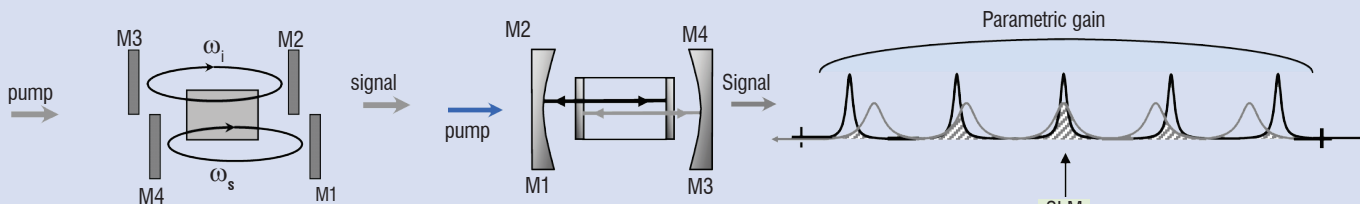


Figure B2 - 03 - Dual-cavity doubly resonant OPO (left); entangled cavities arrangement (right).

Figure B2 - 04 - Principle of the spectral filtering by Vernier effect.

In a dual-cavity doubly resonant OPO, the signal and idler fields experience two different cavities whose optical lengths can be separately adjusted to obtain different free spectral ranges. Doubly resonant oscillation can only take place at discrete spectral positions where there is a mode coincidence between the signal and idler cavities within the parametric gain curve. Thus, single longitudinal mode operation can be achieved if the two cavities lengths are adjusted to get just one mode coincidence. This situation is achieved by choosing slightly different optical lengths. Figure B2-04 illustrates the principle of mode selection that we call 'spectral filtering by Vernier effect'. Experimentally, stable single longitudinal mode operation is obtained if the two cavity lengths differ by 5 to 10%. Once the doubly resonant oscillation has been achieved, the output frequency can be finely tuned by adjusting the two cavities' lengths simultaneously by means of two PZT actuators so as to maintain the mode coincidence during the frequency scanning procedure.

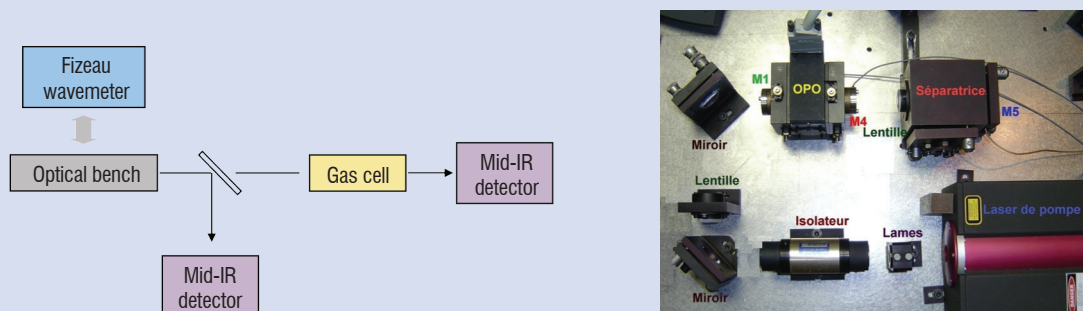


Figure B2-05 : Experimental set-up for absorption spectroscopy; general diagram (left) an optical bench (right)

The potentiality of the dual-cavity doubly resonant OPO for spectroscopic applications has been tested with the experimental set-up depicted in Figure B2 - 05. The pump radiation is produced by a compact passively Q-switched Nd: YAG laser. This commercial laser (Innolight, model Mephisto Q) delivers $20\ \mu\text{J}$ pulses at a 10 kHz repetition rate, the pulse duration is 8 ns. The non linear crystal is a 6 mm-long multi-grating periodically poled lithium niobate (PPLN) providing a tunable idler radiation between 3.8 to $4.2\ \mu\text{m}$. The output coupling of the idler field is obtained through M4, which has a partial reflectivity (70%) around $3.9\ \mu\text{m}$.

In order to perform high resolution absorption spectroscopy, 50% of the idler radiation goes through a 10-cm long absorption cell while 50% is used for power normalization. We get absorption spectra by recording the ratio of the two signals versus the idler wavelength. A Fizeau wavemeter monitors the signal wavelength coming from the OPO.

An absorption spectrum of N_2O at a pressure of 10 hPa is shown in Figure B2-06 as well as the simulated spectrum obtained from the Hitran database. The results demonstrate that absorption spectra can be recorded in continuous, mode-hop-free scans over more than 10 nm. They also illustrate the narrow optical line width delivered by the dual-cavity doubly resonant OPO. This experiment is a preliminary step towards making highly sensitive gas sensors based on optical parametric oscillators.

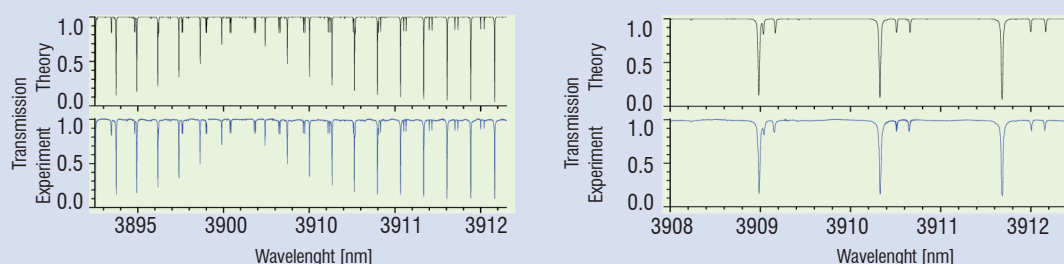


Figure B2 - 06 - N_2O absorption spectrum recorded at 10 hPa (in blue), the high resolution is illustrated by zooming the 3910 nm region (right side); the most-intense absorption lines are attributed to the $2\nu_1$ fundamental vibrational band, whereas the doublets of lines are related to the hot vibrational band ($2\nu_1 + \nu_2 \rightarrow \nu_2$).

References

- [1] J. C. HILL, G.P. MONTGOMERY - *Diode Lasers for Gas Analysis*. Applied Optics, vol.15,n° 3, p.748-755, 1976
- [2] B. ROSIER, D. HENRY, A. COPALLE - *Carbon Monoxide Concentrations and Temperature Measurements in a Low Pressure CH₄-O₂-NH₃ Flame*. Applied Optics, vol.27,n° 2, p.360-364, 1988
- [3] M. P. ARROYO, S. LANGLOIS, R. K. HANSON - *Diode Laser Absorption Technique for Simultaneous Measurements of Multiple Gas Dynamic Parameters in High Speed Flows Containing Water Vapor*. Applied Optics, vol 33, nm15,20 May 1994
- [4] A. K. MOHAMED, B. ROSIER, D. HENRY, Y. LOUVET, P. L. VARGHESE - *Tunable Diode Laser Measurements on Nitric Oxide in a Hypersonic Wind-Tunnel*, AIAA Paper 95-0428
- [5] A. K. MOHAMED, B. ROSIER, P. SAGNIER, D. HENRY, Y. LOUVET, D. BIZE - *Application of Infrared Diode Laser Absorption Spectroscopy to the F4 High Enthalpy Wind Tunnel*. Aerospace Science and Technology, n°4,241-250, 1998
- [6] A. MOHAMED, D. HENRY, J. P. FALÉNI, P. SAGNIER, A. MASSON, W. BECK - *Infrared Diode Laser Absorption Spectroscopy Measurements in the S4MA, F4 and HEG Hypersonic Flows*. International Symposium on Atmospheric Reentry Vehicles and Systems, Arcachon (France), 16-18 March 1999
- [7] W. H. BECK, O. TRINKS, M. WOLLENHAUPT, A. MOHAMED, C. NIEDERBAÜMER, P. ANDRESEN, T. KISHIMOTO, H. BITO - *Probing of the Reservoir, Free Stream and Shock Layers in HEG using Spectroscopic Techniques*. Paper 1350, 21st International symposium on Shock Waves, Great Keppel Island, Australia, July 20-25, 1997
- [8] A. MOHAMED, J.L. VERANT, J. SOUTADÉ, P. VIGUIER, B. VAN OOTEGEM, P. TRAN - *Mid-Infrared Diode Laser Absorption Spectroscopy Measurements in CO-CO₂ Hypersonic Flows of F4 and SIMOUN*. 6th European Symposium on Aerothermodynamics for Space Vehicles, Versailles (France) 3-5 November 2000
- [9] ANATOLIY A. KOSTEREV AND FRANK K. TITTEL - *Chemical Sensors Based on Quantum Cascade Lasers*. IEEE journal of quantum electronics, Vol. 38, no. 6, June 2002
- [10] W. W. BEWLEY, C. L. CANEDY, C. KIM, M. KIM, J. A. NOLDE, D. C. LARRABEE, J. R. LINDLE, I. VURGAFTMAN, AND J. R. MEYER - *Mid-Infrared Interband Cascade Lasers Operating CW at Thermoelectric-Cooler Temperatures*. Conference on Lasers and Electro-Optics/Quantum Electronics and Laser Science Conference and Photonic Applications Systems Technologies, OSA Technical Digest (CD) (Optical Society of America, 2008), paper CTuZ3
- [11] ABDELMAGID SALHI, DAVID BARAT, DANIELE ROMANINI, YVES ROUILLARD, AIMERIC OUVARD, RALPH WERNER, JOCHEN SEUFERT, JOHANNES KOETH, AURORE VICET, AND ARNAUD GARNACHE. *Single-Frequency Sb-based Distributed-Feedback Lasers Emitting at 2.3 μm above Room Temperature for Application in Tunable Diode Laser Absorption Spectroscopy*. Appl. Opt. 45, 4957-4965 (2006)
- [12] A. DESORMEAUX, M. LEFEBVRE, E. ROSENCHER, AND J.-P. HUIGNARD - *Mid-Infrared High-Resolution Absorption Spectroscopy by Use of a Semimonolithic Entangled-Cavity Optical Parametric Oscillator*. Opt. Lett. 29, 2887-2889 (2004)
- [13] G. BERDEN, R. PEETERS, G. MEIJER - *Cavity Ring-Down Spectroscopy: Experimental Schemes and Applications*. International Reviews in Physical Chemistry, Vol. 19, No. 4., pp. 565-607, (2000)
- [14] A. K. MOHAMED - *MSTP Phase 2 Progress Report. Infrared Diode Laser Absorption Spectroscopy in Wind Tunnels*. I-Experimental Setup, II-Data Reduction Procedures (ESA -HT-TN-E34-701&702&703-ONER), Onera Technical Report n° 8 and 9 /7301 PY, 1996.
- [15] L. S. ROTHMAN, et al. *The HITRAN 2008 molecular spectroscopic database*. Journal of Quantitative Spectroscopy and Radiative Transfer, Volume 110, Issues 9-10, Pages 533-572 1992, June-July 2009
- [16] PH. SAGNIER, J. L. VÉRANT - *Flow characterization in the Onera F4 high enthalpy wind tunnel*. AIAA J., Vol.36, N°4, pp.522-531, 1998
- [17] PH. SAGNIER, J. L. VÉRANT - *On the Validation of High Enthalpy Wind Tunnel Simulations*. Aerospace Sciences and Technology, n°7, p. 425-437, 1998
- [18] MENELAS - *Project Final Report*. European Community Contract G4RD-CT-2002-00645, Onera RF 3/07279 DMPH - September 2006
- [19] T. BEHRENDT, C. HASSA, A. MOHAMED, J.-P. FALÉNI - *In situ Measurement and Validation of Gaseous Species Concentrations of a Gas Turbine Model Combustor by Tunable Diode Laser Absorption Spectroscopy (TDLAS)*. Paper GT2008-51258, Proceedings of ASME Turbo Expo 2008, Berlin, Germany, June 9-13, 2008
- [20] H.W. JENTINK, H.P.J. VEERMAN, A.K. MOHAMED AND P. GEISER - *Spectroscopic Measurements of Aircraft Exhaust Gas*, MENELAS Report D 12, National Aerospace Laboratory NLR Report NLR-CR-2006-100, 2006

Acronyms

DLAS (Diode Laser Absorption Spectrometer)

HWHM (Half-Width at Half Maximum)

OPO (Optical Parametric Oscillator)

MIDROPO (Mid-Infrared Doubly Resonant Optical Parametric Oscillator)

MIRPL (Mid-Infrared Pico-second LIDAR)

TDLAS (Tunable Diode Laser Absorption Spectroscopy)

CRDS (Cavity Ring Down Spectroscopy)

AUTHORS



Ajmal Khan Mohamed obtained his Ph.D. in Molecular Physics from the University of PARIS XI in 1991. He then joined the Physics Department of Onera to continue the development of several optical diagnostics (Infrared Diode Laser Absorption Spectroscopy, Electron Beam Fluorescence, Emission Spectroscopy) to probe high enthalpy hypersonic flows in arcjets and shock tubes. He has also been involved in solid state laser development for Laser Induced Fluorescence and in cavity enhanced spectroscopy for trace species detection. He managed several internal or European projects on these techniques for in-flight measurements as well as for environmental applications and is still active in this field of optical diagnostics.



Michel Lefebvre received his Ph.D Degree from the University of Lille I and the Habilitation Degree in Optics from the University of Paris XI. He is currently senior scientist at Onera where he leads the 'Laser Sources and Sensing Physics' research unit in Palaiseau. He conducted various studies in non linear optics and laser sources. He developed and applied the CARS technique to reactive flow and hypersonic wind tunnels. His current research covers parametric conversion processes and optical parametric laser sources.